Journal of Computational Applied Mechanics 2026, 57(3): 526-537

DOI: 10.22059/jcamech.2026.415461.1837

RESEARCH PAPER

A Laplace Transform Approach for Static Analysis of Cracked Axially Functionally Graded Beams with Variable Cross Section

Şeref Doğuşcan AKBAŞ *

Department of Civil Engineering, Bursa Technical University, Mimar Sinan Campus, Bursa, 16310, Turkey

Abstract

This study presents a comprehensive analytical investigation of the static analysis of a cracked axially functionally graded cantilever beam with exponentially varying material properties and cross-sectional geometry in the longitudinal direction. The crack is defined in the system using an equivalent rotational spring model. The main focus of this study is to solve this system, which contains complex discontinuities and variable coefficient differential equations, within a high-precision analytical framework, eliminating the computational cost imposed by numerical methods. Laplace transform method is effectively applied in solving the governing equations. The developed analytical model can express the effect of material gradient and crack stiffness parameters on beam deflection in closed form. The obtained analytical results are compared with exact integration solutions in the literature under different crack stiffness values. This study provides a faster, mathematically stable, and reliable solution method for functionally graded structures compared to traditional numerical methods, thus creating a unique and powerful analytical infrastructure for structural health monitoring and design optimization processes.

Keywords: Functionally Graded Materials; Cracked Beam; Variable Cross-Section Beam; Static Analysis, Laplace Transform

1. Introduction

Cracks encountered by engineering structures throughout their life cycles are critical failure modes that directly affect structural integrity and safety performance. Functionally graded material (FGM), particularly those used in the aerospace and energy sectors, offer high thermal and mechanical resistance due to their gradient structure; however, cracks that may occur in these structures complicate the structural response. Rapid and reliable detection of damage in beam structures constitutes one of the most fundamental areas of study in the discipline of structural health monitoring. Numerous studies exist in the literature on the static and dynamic analysis of cracked beams. Traditional approaches generally rely on finite element methods or solution methods based on complex numerical iterations. However, these methods can lead to high computational costs and limit the speed of parametric analyses in FGM structures where material and geometric changes are continuous.

* Corresponding author. Tel.: +90 224 300 34 98;
E-mail address: serefda@yahoo.com , seref.akbas@btu.edu.tr

In the literature, the vibration, buckling, dynamic stability, and static behavior of cracked FGM beams have been investigated using various theoretical and numerical methods. Furthermore, the mechanical behavior of beams with variable cross-sections and axially functionally graded beams has become a significant research topic in recent years. Khiem and Huyen [1] developed an analytical method for crack detection in functionally graded Timoshenko beams. Rizov [2] investigated the longitudinal behavior of two-dimensional functionally graded cracked beams exhibiting material nonlinearity. Ferezqi et al. [3] presented an analytical approach for the free vibration behavior of cracked functionally graded Timoshenko beams. Gartia et al. [4] analytically performed the free vibration analysis of multi-cracked FGM nanobeams on an elastic basis. Rizov [5] investigated the elastic-plastic longitudinal fracture behavior in functionally graded beams. Akbaş [6] investigated the axially forced vibration behavior of cracked nanorods. Akbaş [7] investigated the bending behavior of cracked functionally graded nanobeams. Maleki and Mohammadi [8] investigated the buckling behavior of cracked FGM columns with piezoelectric patches. Khiem et al. [9] used wavelet transform and artificial neural networks for crack detection in FGM frame systems. Khiem et al. [10] performed crack identification in FGM beams using distributed piezoelectric sensors. Benadouda et al. [11] investigated the effects of porosity and cracks on wave propagation in FGM beams. Dos Santos and Silberschmidt [12] performed finite element analysis of non-uniform multi-cracked FGM Timoshenko beams. Ke et al. [13] investigated the bending vibration and elastic buckling behavior of cracked FGM Timoshenko beams. Yan and Yang [14] investigated the forced vibration behavior of edge-cracked FGM beams under moving load. Akbaş [15] performed free vibration analysis of edge-cracked FGM beams on a Winkler–Pasternak foundation. Yang et al. [16] investigated the free vibration behavior of cracked FGM beams using a continuous beam model. Cunedioglu and Shabani [17] performed the free vibration analysis of symmetric stepped FGM beams with single-edge cracks. Erdurcan and Cunedioglu [18] investigated the free vibration behavior of aluminum beams with damaged FGM cladding. Shabani and Cunedioglu [19] investigated the free vibration analysis of non-uniform symmetric FGM beams. Shabani and Cunedioglu [20] investigated the free vibration behavior of cracked multilayered symmetric sandwich FGM beams. Khoram-Nejad et al. [21] investigated the vibration behavior of cracked axial FGM beams under compressive load. Yang and Chen [22] performed free vibration and buckling analyses of edge-cracked FGM beams. Al Rjoub and Al-Momani [23] investigated the free vibration behavior of axially loaded porous cracked FGM beams. Akbaş [24] performed free vibration analysis of edge-cracked FGM microbeams using modified couple stress theory. Huyen and Khiem [25] investigated the frequency behavior of cracked FGM cantilever beams. Mohcine et al. [26] studied the geometric nonlinear free and forced vibration behavior of discontinuity-containing FGM beams. Chajdi et al. [27] performed geometric nonlinear vibration analysis of multi-cracked FGM beams. Akbaş [28] studied the geometric nonlinear static analysis of edge-cracked FGM Timoshenko beams. Yu and Chu [29] performed crack identification in FGM beams using p-version finite element method. Elaikh and Agboola [30] studied the transverse vibration behavior of axially moving cracked FGM beams under thermal load. Khiem et al. [31] performed modal analysis of cracked continuous FGM Timoshenko beams. Lien et al. [32] investigated the mode shapes of multi-cracked FGM Timoshenko beams. Khiem et al. [33] investigated the natural frequencies of multi-stage cracked FGM beams. Tam et al. [34] investigated the nonlinear bending behavior of graphene-reinforced cracked FGM beams with elastic boundary conditions. Kumar and Panigrahi [35] investigated the nonlinear dynamic behavior of tapered FGM beams with rotating cracks. Song et al. [36] investigated the nonlinear dynamic instability of cracked graphene-reinforced FGM composite beams. Yan et al. [37] investigated the nonlinear dynamic behavior of cracked FGM Timoshenko beams under parameterized excitation. Panigrahi and Pohit [38] investigated the nonlinear dynamic response of open and breathed cracked FGM beams. Panigrahi and Pohit [39] performed a nonlinear dynamic analysis of cracked FGM Timoshenko beams based on a neutral surface approach. Ganguwar and Nistane [40] numerically investigated the crack initiation angle and stress field in cracked FGM beams. Akbaş [41] investigated the post-buckling behavior of edge-cracked FGM beams under axial load. Ke et al. [42] investigated the post-buckling behavior of cracked FGM Timoshenko beams under end shortening effect. Sinha and Kumar [43] presented a comprehensive review of the vibration analysis of cracked FGM structural elements. Mao et al. [44] performed static and dynamic stability analyses of oblique cracked FGM beams. Fu et al. [45] investigated the thermal buckling behavior of FGM beams with longitudinal cracks. Akbaş [46] investigated the wave propagation behavior in FGM beams with edge cracks.

In this study, it is developed to analytically determine the end displacement of a cracked cantilever beam with exponentially varying material properties and cross-sectional geometry. The main originality of the study lies in the use of the Laplace transform method in solving complex differential equations. Unlike traditional methods, this proposed analytical approach successfully models the crack-induced local elasticity effect, along with the material gradient, within a single set of closed-form equations. The obtained results demonstrate that the method is in full agreement with the exact integration results in the literature, covering a wide range from the intact to the deeply cracked condition. In this respect, the study fills a gap in the literature by offering a new analytical solution

framework that is faster, mathematically in-depth, and highly accurate for the analysis of FGM structures.

2. Theory and Formulations

In this study, the static behavior of a cracked cantilever beam, where material properties and cross-sectional geometry vary exponentially along the longitudinal axis, is theoretically modeled. The physical model representing the problem and the rotational spring mechanism used to model the effect of the crack are presented in Figure 1. It is assumed that the beam of length L is fixed at x=0 and subjected to a singular load P at position x_p. The crack at position x_c on the beam is treated as a local flexibility in the structural continuity. The local effect of the crack on the beam rigidity is represented by the rotational spring model. In this model, the discontinuity in the crack cross-section causes an additional rotation angle expressed by the spring constant K. In the following subsections, the governing differential equations of this physical model will be established, and the solution process will be detailed using the Laplace transform technique.

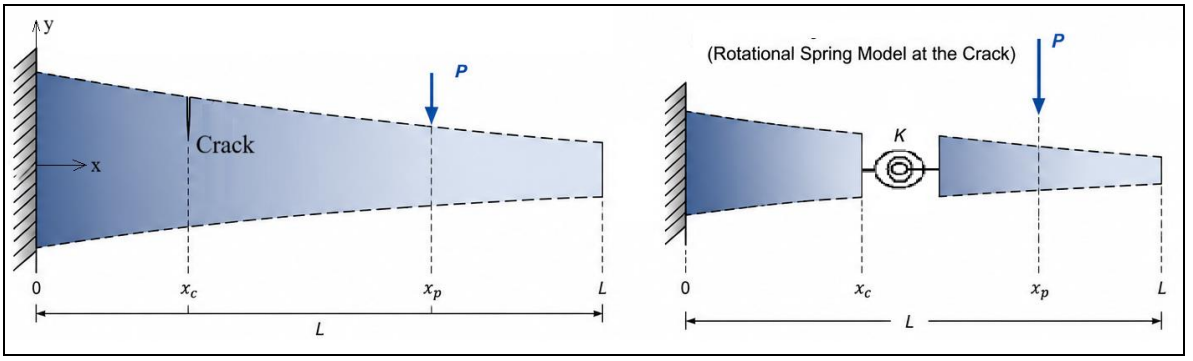

Fig 1: Physical model of axially functionally graded cracked cantilever beam with variable cross section and crack representation using the rotational spring method.

In this study, it is assumed that elasticity modulus E(x) and a cross-sectional area A(x) decrease from the fixed support to the free end as an exponential function given in Equation 1.

$$E(\mathrm{x}) = \mathrm{E}_0 e^{-\alpha x}, \ \alpha > 0 \tag{1a}$$

$$A(\mathrm{x}) = \mathrm{A}_0 e^{-\beta x}, \ \beta > 0 \tag{1b}$$

where α is the material gradient coefficient and β is the cross-sectional area gradient coefficient. E_0 and A_0 represent the modulus of elasticity and cross-sectional areas at x=0 (at the fixed support), respectively. According to Euler-Bernoulli beam theory, the static moment due to the concentrated load at x=x_p in a cracked cantilever beam with axial and geometric variability is zero on the right side of the load ($\mathrm{x}>\mathrm{x}_p$). Using the Heaviside step function (H), the moment (M) for the entire beam is given in the following equation.

$$M(\mathrm{x}) = P(x_p - x)\left[1 - H(x - x_p)\right] = P(x_p - x) + P(x_p - x)H(x - x_p) \tag{2}$$

In the crack model, the displacement (w) at point x_c is continuous, but the slope (w') is not continuous and jumps. According to the spring rotation model at the crack point, the jump of θ_c mathematically means that the curvature (w'') contains a Dirac Delta function (δ) at that point:

$$\frac{d^2w}{dx^2} = \frac{M(\mathrm{x})}{EI(\mathrm{x})} + \theta_c \delta(x - x_c) \tag{3}$$

According to Equation 1, the bending stiffness of the beam, EI(x), is expressed as follows.

$$EI(\mathrm{x}) = \mathrm{E}_0\mathrm{I}_0 e^{-(\alpha+\beta)x} = \mathrm{E}_0\mathrm{I}_0 e^{-\gamma x} \tag{4}$$

where I_0 is section moment of inertia at the point x=0, γ= α+β which is expressed as the total gradient coefficient of the beam. If the moment function in equation (2) and the bending stiffness expressions in equation (4) substitute into

the governing differential equation in equation (3), the governing differential equation for the problem is obtained in the following equation.

$$\frac{d^2w}{dx^2} = \frac{P(x_p-x)+P(x_p-x)H(x-x_p)}{E_0 I_0 e^{-\gamma x}} + \theta_c \delta(x-x_c) \tag{5}$$

If the constant $D=P/E_0I_0$ is defined, the equation in (5) is rewritten as follows.

$$\frac{d^2w}{dx^2} = Dx_p e^{\gamma x} - Dxe^{\gamma x} + D(x-x_p)e^{\gamma x}H(x-x_p) + \theta_c \delta(x-x_c) \tag{6}$$

Laplace transform of the displacement function $w(x)$ in the s-domain is $\mathcal{L}\{w(x)\} = W(s)$. Since the boundary conditions at the fixed support (x=0) are $w(0)$=0 and $w'(0)$ = 0, the transformation of the left side of the differential equation in equation (6) is $\mathcal{L}\{w''(x)\} = s^2W(s)$. The rearrangement of the lagged (Heaviside) term on the right side to the s-domain by applying Laplace's second shift theorem is presented in the operations in the following equation.

$$\begin{aligned}(x-x_p)e^{\gamma x}H(x-x_p) &= (x-x_p)e^{\gamma(x-x_p+x_p)}H(x-x_p) \\ &= e^{\gamma x_p}\left[(x-x_p)e^{\gamma(x-x_p)}\right]H(x-x_p)\end{aligned} \tag{7}$$

When the expression obtained in equation (7) is written in equation (6), the governing differential equation of the problem is rewritten in the following equation.

$$\frac{d^2w}{dx^2} = Dx_p e^{\gamma x} - Dxe^{\gamma x} + D\, e^{\gamma x_p}\left[(x-x_p)e^{\gamma(x-x_p)}\right]H(x-x_p) + \theta_c \delta(x-x_c) \tag{8}$$

Applying the Laplace transform to the differential equation in equation (8) and dividing each side by s^2, the following expression is obtained.

$$W(s) = Dx_p\left[\frac{1}{s^2(s-\gamma)}\right] - D\left[\frac{1}{s^2(s-\gamma)^2}\right] + De^{\gamma x_p}\left[\frac{e^{-sx_p}}{s^2(s-\gamma)^2}\right] + \theta_c\left[\frac{e^{-sx_c}}{s^2}\right] \tag{9}$$

To return the system to real space, the inverse Laplace counterparts of the rational expressions within each bracket are presented in the following equations:

$$\mathcal{L}^{-1}\left\{\frac{1}{s^2(s-\gamma)}\right\} = -\frac{1}{\gamma^2} - \frac{x}{\gamma} + \frac{e^{\gamma x}}{\gamma^2} = f_1(x) \tag{10a}$$

$$\mathcal{L}^{-1}\left\{\frac{1}{s^2(s-\gamma)^2}\right\} = \frac{2}{\gamma^3} + \frac{x}{\gamma^2} - \frac{2\,e^{\gamma x}}{\gamma^3} + \frac{x\,e^{\gamma x}}{\gamma^2} = f_2(x) \tag{10b}$$

$$\mathcal{L}^{-1}\left\{\frac{e^{-sx_p}}{s^2(s-\gamma)^2}\right\} = f_2(x-x_p)H(x-x_p) \tag{10c}$$

$$\mathcal{L}^{-1}\left\{\frac{e^{-sx_c}}{s^2}\right\} = (x-x_c)H(x-x_c) \tag{10d}$$

When you substitute the inverse transformation components, the overall solution appears as follows:

$$W(x) = Dx_p f_1(x) - Df_2(x) + De^{\gamma x_p} f_2(x-x_p)H(x-x_p) + \theta_c(x-x_c)H(x-x_c) \tag{11}$$

When the displacement function in equation (11) is written in its explicit form and factored out, the following equation is obtained.

$$W(x) = D\left[e^{\gamma x}\left(\frac{x_p}{\gamma^2}+\frac{2}{\gamma^3}\right)-\frac{xe^{\gamma x}}{\gamma^2}-x\left(\frac{x_p}{\gamma}+\frac{1}{\gamma^2}\right)-\left(\frac{x_p}{\gamma^2}+\frac{2}{\gamma^3}\right)\right] + De^{\gamma x_p}\left[\frac{2}{\gamma^3}+\frac{x-x_p}{\gamma^2}-\frac{2e^{\gamma(x-x_p)}}{\gamma^3}+\frac{(x-x_p)e^{\gamma(x-x_p)}}{\gamma^2}\right]H(x-x_p) + \theta_c(x-x_c)H(x-x_c) \quad (12)$$

The relationship between the crack location x_c and the load location x_p determines the characteristics of this problem. In the Rotational Spring Model used at the crack point, the amount of rotation at the crack point is directly proportional to the internal moment acting on that point.

$$\theta_c = \frac{M(x_c)}{K} \quad (13)$$

If the crack is between the fixed support and the load, it is directly affected by the moment. The external moment at point $x=x_c$ is $M(x_c) = P\,(x_p - x_c)$. In this case, the relationship between moment and rotation amount at the crack point is as shown in the following equation.

$$\theta_c = \frac{P(x_p - x_c)}{K} \quad (14)$$

If the crack is to the right of the load ($x_c > x_p$), the section moment at the crack point is zero. In this case, the crack does not open at all and does not add any flexibility to the beam displacement formula. To combine these two situations into a single mathematical expression, the Heaviside function can be used:

$$\theta_c = \frac{P(p - x_c)}{K}H(x_p - x_c) \quad (15)$$

Substituting the expression θ_c from Equation 15 and the constant $D=P/E_0I_0$ into Equation (12), the complete displacement solution of the exponentially narrowed cross-section cantilever beam with an exponentially axial functional grade, containing load and crack at an arbitrary position, is as shown in the following equation.

$$W(x) = \frac{P}{E_0I_0}\left[e^{\gamma x}\left(\frac{x_p}{\gamma^2}+\frac{2}{\gamma^3}\right)-\frac{xe^{\gamma x}}{\gamma^2}-x\left(\frac{x_p}{\gamma}+\frac{1}{\gamma^2}\right)-\left(\frac{x_p}{\gamma^2}+\frac{2}{\gamma^3}\right)\right]+\frac{P}{E_0I_0}e^{\gamma x_p}\left[\frac{2}{\gamma^3}+\frac{x-x_p}{\gamma^2}-\frac{2e^{\gamma(x-x_p)}}{\gamma^3}+\frac{(x-x_p)e^{\gamma(x-x_p)}}{\gamma^2}\right]H(x-x_p)+\frac{P(p-x_c)}{K}H(x_p-x_c)(x-x_c)H(x-x_c) \quad (16)$$

Dimensionless expressions are used in the numerical results of the study. The dimensionless expressions and parameters used are presented in the following equation.

$$\xi = \frac{x}{L}, 0 \le \xi \le 1, \quad \xi_c = \frac{x_c}{L},\ \xi_p = \frac{x_p}{L},\ \bar{w} = \frac{w\,E_0I_0}{PL^3},\ \Gamma = (\alpha+\beta)L = \gamma L,\ K_T = \frac{KL}{E_0I_0} \quad (17)$$

where ξ represents the dimensionless length, ξ_c the dimensionless crack position, ξ_p the dimensionless load position, $\bar{w}$ the dimensionless displacement, Γ the dimensionless total gradient parameter, and K_T the dimensionless spring stiffness. It should be noted that as K_T approaches infinity ($K_T \to \infty$), the beam transforms into intact state, and as K_T approaches zero ($K_T \to 0$), a hinged beam state is formed. If the gradient parameter $\Gamma=0$, the beam has a homogeneous and constant cross-section.

3. Numerical Results and Discussion

This section presents numerical applications of the analytical model developed for the analysis of end displacements of cracked axially functionally graded beams with variable cross section. The main objective of the study is to comprehensively investigate the effects of fundamental variables such as dimensionless crack position

(ξ_c), dimensionless load position (ξ_p), dimensionless crack stiffness (K_T), and gradient parameter (Γ), representing the dimensionless gradient of the material and geometry, on the static response of the beam. During the analyses, the geometric continuity of the beam is preserved, and the crack effect is integrated as a singular discontinuity defined in the system's governing equations using Laplace transform. In the numerical calculations, the material and geometric properties of the beam are normalized using standard dimensionless values consistent with the literature. In the solution of the equations and obtaining the numerical results and graphs, necessary algorithms and programs are created in Scilab program. To ensure the consistency of the study, unless otherwise specified, the gradient parameter (Γ) is kept constant at 0.5, and the crack stiffness (K_T) values are selected within a range of 1 to 20 to reflect the degree of structural damage. Furthermore, a complete parametric scan is performed along the beam by normalizing the load location (ξ_p) and crack location (ξ_c) within the range of 0 to 1. The results show that the proposed analytical method successfully simulates the local elasticity changes caused by cracks and the global deflection characteristics of these changes reflected at the beam endpoint.

To verify the accuracy of the proposed analytical model, the dimensionless free-end displacement results obtained based on crack stiffness (K_T) values are compared with the reference values obtained by the analytical exact integration method of the differential equation for a homogeneous and constant cross-section beam (for Γ=0). In this validation study, the load is taken at the free end (ξ_p =1) and the crack location at the midpoint (ξ_c=0.5). The dimensionless vertical displacement function of a homogeneous and constant cross-section cantilever beam with a crack at the midpoint (ξ_c=0.5) and a concentrated load at the free end (ξ_p=1) is calculated in dimensionless coordinates ξ as $w(\xi) = \xi_p^2(3-\xi_p)/6 + (\xi_p - \xi_c)(1-\xi_c)/K_T$ using the analytical exact integration method of the differential equation.

Table 1 compares the dimensionless vertical displacement ($w(1)$) values at the free end of the cantilever beam. As seen in Table 1, the values obtained from the proposed Laplace-based model and the results obtained from the analytical exact integration method show complete agreement across all crack stiffness (K_T) ranges. This complete overlap proves the accuracy of the mathematical basis of our developed model and its superior sensitivity in modeling the behavior of cracked systems.

Table 1: Comparison of the results of the developed Laplace transform-based model with the analytical exact integration solution for homogeneous and constant cross-section beam. Dimensionless vertical displacement values at the free end.

K_T	Exact Integration Solution	Present (With Laplace Transformation)
0.5	0.83333	0.83333
1	0.58333	0.58333
5	0.38333	0.38333
10	0.35833	0.35833
Intact (∞)	0.33333	0.33333

Figures 2a and 2b illustrate the relationship between the dimensionless gradient parameter Γ and the dimensionless displacement of free end for different crack and load locations, over different K_T values (crack depths). This analysis is performed to define the interaction between the functionally graded material properties of the beam and the crack parameters. Figure 2a shows the results for the case where the point of application of the load is further to the left of the crack point ($\xi_c > \xi_p$) (for ξ_c =0.5, ξ_p=0.3), while Figure 2b shows the results for the case where the point of application of the load is further to the right of the crack point ($\xi_c < \xi_p$) (for ξ_c =0.5, ξ_p=1).

As seen in both graphs in Figures 2a and 2b, as the gradient parameter (Γ) increases, the end displacement exhibits a linear increase trend due to changes in the material's stiffness characteristics. This demonstrates that the gradient structure is decisive in determining the overall flexibility of the beam. In Figure 2a, where the load lags behind the crack ($\xi_c > \xi_p$), the difference between the K_T values (1, 5, and 10) almost disappears. This indicates that the beam's response is largely governed by the gradient parameter, as the crack effect has not yet fully come into play. In Figure 2b, where the load passes through the crack ($\xi_c < \xi_p$), the difference between the K_T values becomes more pronounced. The case of K_T=1 (larger/deeper crack) results in much higher displacements compared to the others. This reveals that the crack effect becomes dominant on displacement when the load position passes through the crack. In the graphs, a significant increase in displacement values is observed as the K_T value decreases (i.e., as the crack depth increases). It has been analyzed that the displacement capacity of the system is quite sensitive to crack stiffness, especially when the load is ahead of the crack ($\xi_c < \xi_p$).

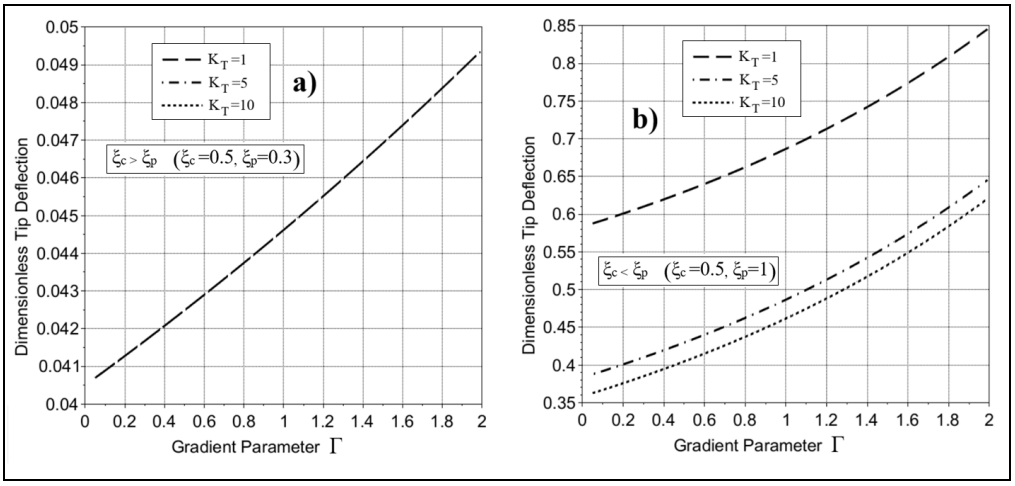

Fig 2: Effect of gradient parameter Γ and dimensionless crack stiffness K_T values on dimensionless tip displacement: a) $\xi_c > \xi_p$ case (ξ_c=0.5, ξ_p=0.3) and b) $\xi_c < \xi_p$ case (ξ_c=0.5, ξ_p=1).

Figure 3 shows how the relationship between load location (ξ_p) and dimensionless end displacement changes for different crack locations (ξ_c=0.1, 0.3, 0.5, 0.8) with K_T=5 and Γ=0.5 values. This graph is presented to analyze the modulation effect of the proximity or distance of the crack to the supports on the overall deflection characteristics of the beam.

As shown in Figure 3, a significant decrease in tip displacement is observed as the crack location moves further away from the support (beam origin) (from ξ_c=0.1 to 0.8). When the crack is at ξ_c=0.1 (close to the support), the total flexibility of the beam is maximized, and the highest displacement values are obtained. As the load propagates along the beam (increase in ξ_p), the tip displacement shows a non-linear (curvilinear) increase in all crack scenarios. When the crack is close to the support (ξ_c= 0.1), the deflection curve formed when the load reaches the beam end exhibits a steeper acceleration compared to other crack locations. These results prove that the crack location directly determines the "damage susceptibility" of the beam. The location of the crack in the middle or end regions of the beam alters the effect of the load on the beam at different "fracture points". Particularly in the ξ_p> 0.6 range, the widening of the shear between the curves representing different crack locations reveals that sensitivity to crack location becomes more pronounced as the load approaches the end of the beam.

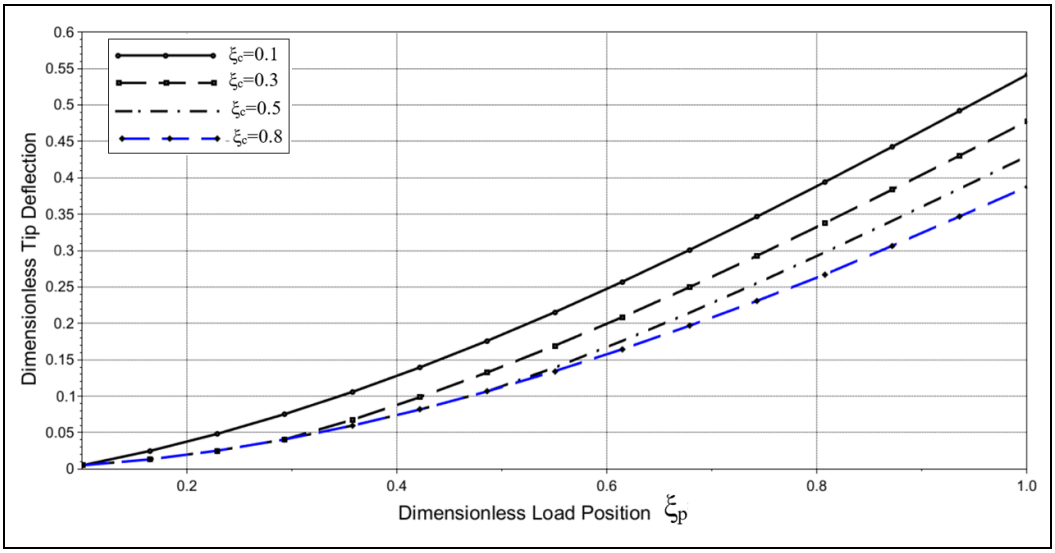

Fig 3: Effect of load positions ξ_p on dimensionless tip displacement for different values of crack position ξ_c.

Figure 4 presents the dependence between crack location (ξ_c=0.1 to 0.9 range) and dimensionless tip displacement for different constant load positions (ξ_p= 0.2, 0.5, 0.7, 1.0) with K_T=5 and Γ=0.5. This analysis reveals how the beam end displacement tends as the crack moves away from the support and how this tendency changes under different loading scenarios.

All the curves in figure 4 show a decreasing trend in end displacement as the crack location (ξ_c) increases from the support (from 0.1 to 0.9). Displacement values are maximum, especially in regions where the crack is close to the support (ξ_c= 0.1). This proves that the elasticity created by the crack near the support is much more dominant on the total deflection capacity of the beam. As the load location (ξ_p) increases, a significant increase in tip displacement values is observed. In scenarios where the load approaches the free end of the beam (ξ_p= 1.0), the "error margin" or "sensitivity range" of the crack location on end displacement is much wider. In cases where the load is in the middle or at the beginning of the beam (ξ_p = 0.2, 0.5), the effect of the crack location is damped after a certain point (approximately ξ_c> 0.5), and the curves flatten out. These findings indicate that the location of the crack in the first half of the beam (regions near the support) plays a more critical role in structural integrity, independent of the load. Crack displacement towards the end of the beam (high ξ_c values) has only marginal effects on the end displacement. This graph visualizes the critical interaction between the progression of the load along the beam and the location of the failure point.

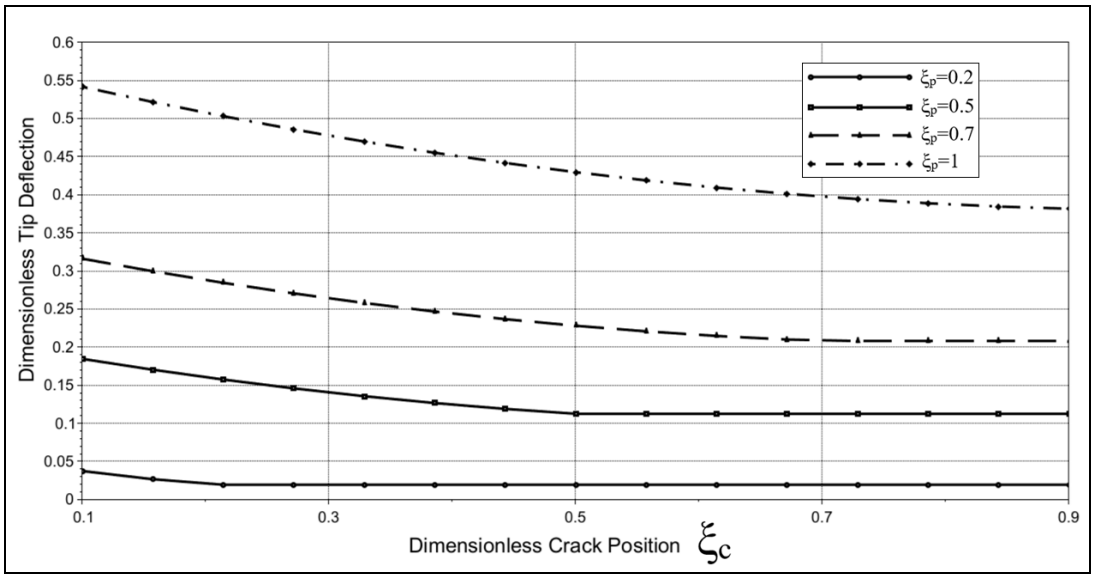

Fig 4: Effect of crack position ξ_c on dimensionless tip displacement under constant load positions ξ_p.

Figures 5a and 5b present the non-linear relationship between the variation of the crack stiffness parameter K_T (inverse of crack depth) and the dimensionless tip displacement for a value of Γ=0.5. In Figure 5a, the effect of crack position (ξ_c) is analyzed parametrically, and in Figure 5b, the effect of load position (ξ_p) is analyzed parametrically. These graphs show how the displacement capacity of the system increases dramatically as the crack depth increases (as the K_T value decreases), and how the system achieves asymptotic stability after a certain KT value.

As shown in Figure 5, an exponential increase in tip displacement is observed as the K_T value decreases (i.e., as the crack depth increases). Specifically, the range $1 \leq K_T \leq 5$ has been defined as the "critical region," where the structure is most susceptible to damage and displacement values increase rapidly. As the K_T value rises to 10 and above, the displacement curves flatten, exhibiting asymptotic behavior. This demonstrates that as the crack depth decreases, the structure approaches "intact beam" behavior, and the crack effect becomes negligible. As shown in Figure 5a, the closer the crack is to the support (ξ_c = 0.2), the more sensitive the system is to K_T changes. As the crack moves away from the support (ξ_c = 0.8), the curves overlap and stabilize at a lower displacement level, independent of K_T changes. As shown in Figure 5b, as the load approaches the free end (ξ_p = 0.8), the end

displacement becomes much more sensitive to changes in crack stiffness. However, when the load is close to the support (ξ_p = 0.2), crack stiffness makes almost no significant difference to the total displacement.

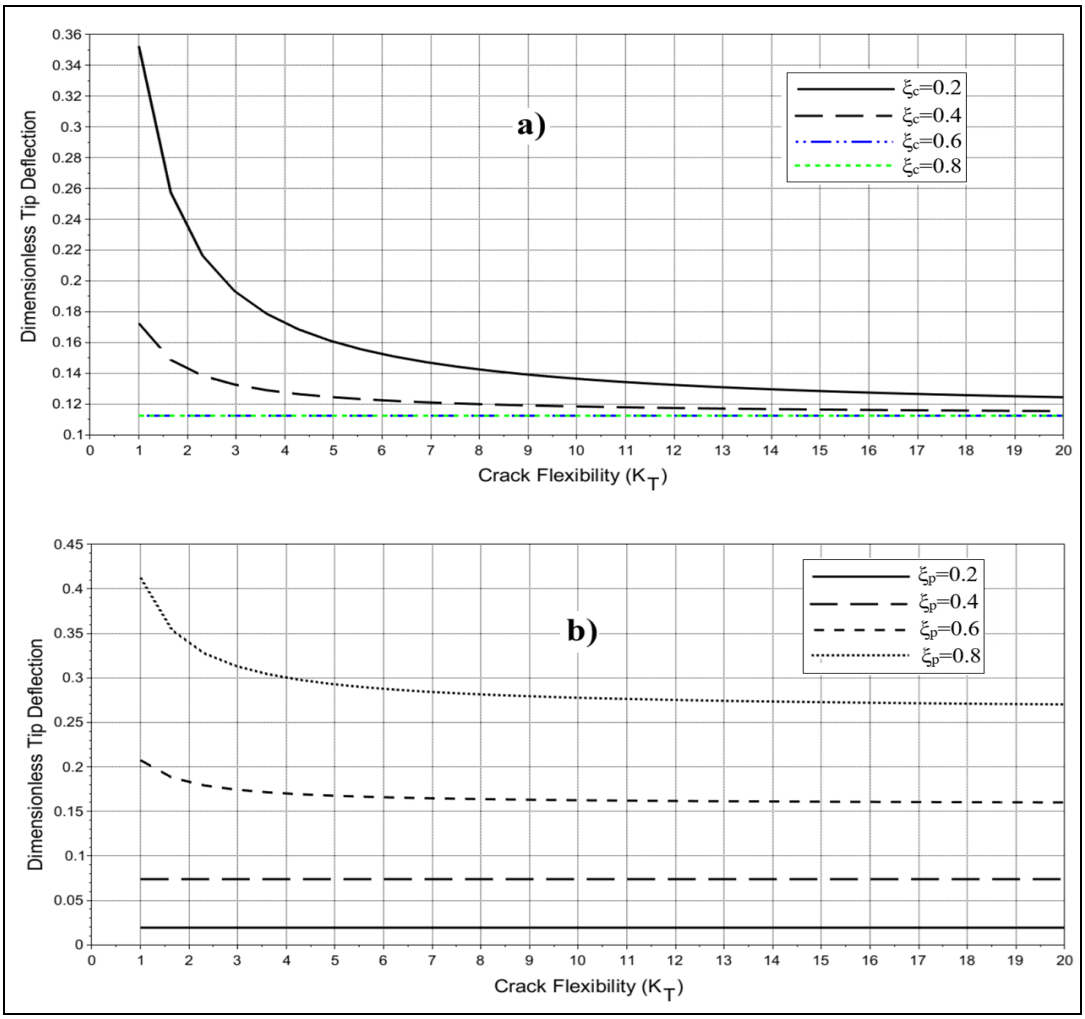

Fig 5: Effect of crack stiffness parameter K_T on dimensionless tip displacement: a) For different crack locations (ξ_c), b) For different load locations (ξ_p).

4. Conclusions

This study presents a novel analytical model based on the Laplace transform for determining the static displacements of fractured axially functionally graded beams. The proposed model combines the mathematical ease provided by the Laplace transform in solving complex differential equations with the physical realities of structural mechanics. The analysis results support the hypotheses set forth at the beginning of the study with the following key findings:

• The governing differential equations of the beam have been transformed into algebraic equations in the Laplace plane (s-plane). This has allowed boundary value problems to be solved directly without the need for complex integration processes.

• The discontinuity effect of the crack on the beam can be easily defined as a "delta function" or "shifting theorem" in the Laplace plane. This eliminates the need to perform separate solutions for cracked and intact regions, allowing the entire system to be expressed by a single set of equations.

• Unlike numerical methods, the used analytical model presents the solution in closed form. The point displacement expressions obtained from the inverse Laplace transform produce results with high accuracy, even under high-frequency or short-duration loading conditions, without exhibiting numerical instability.

• The crack elasticity parameter (KT) has an exponential effect on displacement as an indicator of crack depth. High sensitivity in the range of KT ≤ 5 demonstrates that the method possesses the necessary sensitivity for damage detection.

• The gradient parameter (Γ) modulates the overall stiffness of the beam, determining the "visibility" of the crack effect on the end displacement. The model can successfully isolate this gradient effect.

• The proximity of the crack to the support ($\xi c < 0.3$) maximizes the damage susceptibility. The method successfully captures the "fracture" behavior in the tip displacement when the live load (ξp) passes through the crack, thus establishing the loading and damage interaction on accurate physical grounds.

• In future studies, adapting this model to time-dependent (dynamic) loading and multiple crack scenarios will further expand the applicability of the method.

References

[1] N. T. Khiem, N. N. Huyen, A method for crack identification in functionally graded Timoshenko beam, *Nondestructive Testing and Evaluation,* Vol. 32, No. 3, pp. 319–341, 2017.

[2] V. Rizov, Analysis of longitudinal cracked two-dimensional functionally graded beams exhibiting material non-linearity, *Fracture and Structural Integrity,* Vol. 11, No. 41, pp. 491–503, 2017.

[3] H. Z. Ferezqi, M. Tahani, H. E. Toussi, Analytical Approach to Free Vibrations of Cracked Timoshenko Beams Made of Functionally Graded Materials, *Mechanics of Advanced Materials and Structures,* Vol. 17, No. 5, pp. 353–365, 2010.

[4] A. K. Gartia, P. Rao, S. Chakraverty, Analytical Solution for Free Vibration of Multi-Cracked Metal–Ceramic Functionally Graded Nanobeams Resting on Elastic Foundations, *International Journal of Structural Stability and Dynamics*, pp. 2650400, 2025.

[5] V. Rizov, Analytical study of elastic-plastic longitudinal fracture in a functionally graded beam, *Strength, Fracture and Complexity,* Vol. 10, No. 1, pp. 11–22, 2017.

[6] Ş. D. Akbaş, Axially forced vibration analysis of cracked a nanorod, *Journal of Computational Applied Mechanics,* Vol. 50, No. 1, pp. 63–68, 2019.

[7] Ş. D. Akbaş, Bending of a cracked functionally graded nanobeam, *Advances in Nano Research,* Vol. 6, No. 3, pp. 219–243, 2018.

[8] V. A. Maleki, N. Mohammadi, Buckling analysis of cracked functionally graded material column with piezoelectric patches, *Smart Materials and Structures,* Vol. 26, No. 3, pp. 035031, 2017.

[9] N. T. Khiem, T. Van Lien, N. T. Duc, Crack identification in functionally graded material framed structures using stationary wavelet transform and neural network, *Journal of Zhejiang University-Science A,* Vol. 22, No. 8, pp. 657–671, 2021.

[10] N. T. Khiem, T. T. Hai, L. Q. Huong, Crack identification of functionally graded beam using distributed piezoelectric sensor, *Journal of Vibration and Control,* Vol. 29, No. 15-16, pp. 3401–3417, 2023.

[11] M. Benadouda, M. El Amin Bourouis, M. Dahmane, R. Bennai, H. Ait Atmane, O. Safer, Dynamic response of wave propagation in functionally graded beams with defects: effects of porosity and cracks, *Acta Mechanica,* Vol. 236, No. 3, pp. 2279–2296, 2025.

[12] H. A. Freixial Argente dos Santos, V. V. Silberschmidt, Finite element analysis of non-uniform functionally graded multi-cracked Timoshenko beams using an equilibrium-based formulation, 2026.

[13] L.-L. Ke, J. Yang, S. Kitipornchai, Y. Xiang, Flexural Vibration and Elastic Buckling of a Cracked Timoshenko Beam Made of Functionally Graded Materials, *Mechanics of Advanced Materials and Structures,* Vol. 16, No. 6, pp. 488–502, 2009.

[14] T. Yan, J. Yang, Forced Vibration of Edge-Cracked Functionally Graded Beams Due to a Transverse Moving Load, *Procedia Engineering,* Vol. 14, pp. 3293–3300, 2011.

[15] Ş. D. Akbaş, Free Vibration Analysis of Edge Cracked Functionally Graded Beams Resting On Winkler-Pasternak Foundation, *International Journal of Engineering and Applied Sciences,* Vol. 7, No. 3, pp. 1–15, 2015.

[16] E. C. Yang, X. Zhao, Y. H. Li, Free Vibration Analysis for Cracked FGM Beams by Means of a Continuous Beam Model, *Shock and Vibration,* Vol. 2015, No. 1, pp. 197049, 2015.
[17] Y. Cunedioglu, S. Shabani, Free vibration analysis of a single edge cracked symmetric functionally graded stepped beams, *Advances in Structural Engineering,* Vol. 23, No. 16, pp. 3415–3428, 2020.
[18] E. F. Erdurcan, Y. Cunedioğlu, Free vibration analysis of an aluminum beam coated with imperfect and damaged functionally graded material, *Archive of Applied Mechanics,* Vol. 91, No. 4, pp. 1729–1737, 2021.
[19] S. Shabani, Y. Cunedioglu, Free vibration analysis of cracked functionally graded non-uniform beams, *Materials Research Express,* Vol. 7, No. 1, pp. 015707, 2020.
[20] S. Shabani, Y. Cunedioglu, Free Vibration Analysis of Functionally Graded Beams with Cracks, *Journal of Applied and Computational Mechanics,* Vol. 6, No. 4, pp. 908–919, 2020.
[21] E. Sh Khoram-Nejad, S. Moradi, M. Shishesaz, Free vibration analysis of the cracked post-buckled axially functionally graded beam under compressive load, *Journal of Computational Applied Mechanics,* Vol. 52, No. 2, pp. 256–270, 2021.
[22] J. Yang, Y. Chen, Free vibration and buckling analyses of functionally graded beams with edge cracks, *Composite Structures,* Vol. 83, No. 1, pp. 48–60, 2008.
[23] Y. S. Al Rjoub, M. A. Al-Momani, Free Vibration of Axially Loaded Functionally Graded Porous Cracked Beams, *International Journal of Structural Stability and Dynamics,* Vol. 25, No. 06, pp. 2550058, 2025.
[24] Ş. D. Akbaş, Free Vibration of Edge Cracked Functionally Graded Microscale Beams Based on the Modified Couple Stress Theory, *International Journal of Structural Stability and Dynamics,* Vol. 17, No. 03, pp. 1750033, 2017.
[25] N. N. Huyen, N. T. Khiem, Frequency analysis of cracked functionally graded cantilever beam, *Vietnam Journal of Science and Technology,* Vol. 55, No. 2, pp. 229–243, 2017.
[26] C. Mohcine, M. E. Bekkaye, E. B. Khalid, Geometrically Non-Linear Free and Forced Vibration of Clamped-Clamped Functionally Graded Beam with Discontinuities, *Procedia Engineering,* Vol. 199, pp. 1870–1875, 2017.
[27] M. Chajdi, A. Adri, K. E. Bikri, R. Benamar, Geometrically nonlinear free and forced vibrations analysis of clamped-clamped functionally graded beams with multicracks, *MATEC Web of Conferences,* Vol. 211, pp. 02002, 2018.
[28] Ş. D. Akbaş, Geometrically Nonlinear Static Analysis of Edge Cracked Timoshenko Beams Composed of Functionally Graded Material, *Mathematical Problems in Engineering,* Vol. 2013, No. 1, pp. 871815, 2013.
[29] Z. Yu, F. Chu, Identification of crack in functionally graded material beams using the *p*- version of finite element method, *Journal of Sound and Vibration,* Vol. 325, No. 1, pp. 69–84, 2009.
[30] T. E. Elaikh, O. O. O. Agboola, Investigation of Transverse Vibration Characteristics of Cracked Axially Moving Functionally Graded Beam Under Thermal Load, *Trends in Sciences,* Vol. 19, No. 23, pp. 1349–1349, 2022.
[31] N. T. Khiem, H. T. Tran, D. Nam, Modal analysis of cracked continuous Timoshenko beam made of functionally graded material, *Mechanics Based Design of Structures and Machines,* Vol. 48, No. 4, pp. 459–479, 2020.
[32] T. V. Lien, N. T. Đuc, N. T. Khiem, Mode Shape Analysis of Multiple Cracked Functionally Graded Timoshenko Beams, *Latin American Journal of Solids and Structures,* Vol. 14, pp. 1327–1344, 2017.
[33] N. T. Khiem, T. V. Lien, V. T. A. Ninh, Natural Frequencies of Multistep Functionally Graded Beam with Cracks, *Iranian Journal of Science and Technology, Transactions of Mechanical Engineering,* Vol. 43, No. 1, pp. 881–916, 2019.
[34] M. Tam, Z. Yang, S. Zhao, H. Zhang, Y. Zhang, J. Yang, Nonlinear bending of elastically restrained functionally graded graphene nanoplatelet reinforced beams with an open edge crack, *Thin-Walled Structures,* Vol. 156, pp. 106972, 2020.
[35] G. D. Kumar, B. Panigrahi, Nonlinear dynamic analysis on centrifugal stiffening of rotating cracked tapered functionally graded beam for flap-wise vibrations, *Journal of Vibration and Control,* Vol. 30, No. 9-10, pp. 2154–2170, 2024.
[36] M. Song, L. Zhou, W. Karunasena, J. Yang, S. Kitipornchai, Nonlinear dynamic instability of edge-cracked functionally graded graphene-reinforced composite beams, *Nonlinear Dynamics,* Vol. 109, No. 4, pp. 2423–2441, 2022.
[37] T. Yan, J. Yang, S. Kitipornchai, Nonlinear dynamic response of an edge-cracked functionally graded Timoshenko beam under parametric excitation, *Nonlinear Dynamics,* Vol. 67, No. 1, pp. 527–540, 2012.

[38] B. Panigrahi, G. Pohit, Nonlinear dynamic response of open and breathing cracked functionally graded beam under single and multi-frequency excitation, *Engineering Structures,* Vol. 242, pp. 112437, 2021.

[39] B. Panigrahi, G. Pohit, Nonlinear modelling and dynamic analysis of cracked Timoshenko functionally graded beams based on neutral surface approach, *Proceedings of the Institution of Mechanical Engineers, Part C: Journal of Mechanical Engineering Science,* Vol. 230, No. 9, pp. 1486–1497, 2016.

[40] S. Ganguwar, V. M. Nistane, Numerical Study on the Determination of Crack Initiation Angle, Stress Field and Stress Triaxiality at Crack Tip in a Cracked Beam of Functionally Graded Material, *Journal of Failure Analysis and Prevention,* Vol. 24, No. 6, pp. 2847–2862, 2024.

[41] Ş. D. Akbaş, On Post-Buckling Behavior of Edge Cracked Functionally Graded Beams Under Axial Loads, *International Journal of Structural Stability and Dynamics,* Vol. 15, No. 04, pp. 1450065, 2015.

[42] L.-L. Ke, J. Yang, S. Kitipornchai, Postbuckling analysis of edge cracked functionally graded Timoshenko beams under end shortening, *Composite Structures,* Vol. 90, No. 2, pp. 152–160, 2009.

[43] G. P. Sinha, B. Kumar, Review on Vibration Analysis of Functionally Graded Material Structural Components with Cracks, *Journal of Vibration Engineering & Technologies,* Vol. 9, No. 1, pp. 23–49, 2021.

[44] J.-J. Mao, Y.-J. Wang, J. Yang, Static and Dynamic Stability Analyses of Functionally Graded Beam with Inclined Cracks, *International Journal of Structural Stability and Dynamics,* Vol. 23, No. 16n18, pp. 2340012, 2023.

[45] Y. Fu, Y. Chen, P. Zhang, Thermal buckling analysis of functionally graded beam with longitudinal crack, *Meccanica,* Vol. 48, No. 5, pp. 1227–1237, 2013.

[46] Ş. D. Akbaş, Wave propagation in edge cracked functionally graded beams under impact force, *Journal of Vibration and Control,* Vol. 22, No. 10, pp. 2443–2457, 2016.